The integral Eq. (5) was solved by Lighthill,[6] and its solution is

$$h(\bar{t}) = w_1(\bar{t}) - \int_0^{\bar{t}} S_1(\bar{t} - \bar{s}) w_1(\bar{s}) d\bar{s} \tag{13}$$

Here,

$$w_1(\bar{t}) = \frac{2^{1/2}}{\pi}\left[\frac{g_1(0)}{\bar{t}^{1/2}} + \int_0^{\bar{t}} \frac{g_1'(\bar{x})d\bar{x}}{(\bar{t} - \bar{x})^{1/2}}\right] \tag{14}$$

with $g_1(\bar{x}) = R'(x)/\alpha$, and S_1 the resolvent for $K_1'(z)$. $K_1'(z)$ is the differentiation of $K_1(z)$, and

$$K_1(z) = \frac{2^{3/2}}{\pi}\left\{(2+z)^{1/2}E_1\left[\left(\frac{z}{2+z}\right)^{1/2}\right] - \frac{1}{(2+z)^{1/2}}F_1\left[\left(\frac{z}{2+z}\right)^{1/2}\right]\right\} \tag{15}$$

where E_1 and F_1 are the complete elliptic integrals. Both $K_1'(z)$ and $S_1(z)$ are tabulated in Table 1 [part of $S_1(z)$ data was obtained previously by Lighthill[6]].

Having obtained the source distribution of the streamtube in terms of the disturbances on the streamtube, we may find the F function of this streamtube in terms of these disturbances. By substituting Eq. (12) into the nondimensional form of Eq. (1), we obtain

$$\frac{F(\bar{y})}{(\alpha R)^{1/2}} = \int_0^{\bar{y}} w(\bar{t})T(\bar{y} - \bar{t})d\bar{t} \tag{16}$$

with

$$T(z) = \frac{1}{z^{1/2}} - \int_0^z \frac{S(z - z_1)}{z_1^{1/2}}dz_1 \tag{17}$$

Since $w(\bar{t})$ and $g(\bar{t})$ are also related by Eq. (14), then

$$\frac{F(\bar{y})}{(2\alpha R)^{1/2}} = g(0)U(\bar{y}) + \int_0^{\bar{y}} g'(\bar{x})U(\bar{y} - \bar{x})d\bar{x} \tag{18}$$

where

$$U(\bar{y}) = \frac{1}{\pi}\int_0^{\bar{y}} \frac{T(\bar{y} - \bar{t})}{\bar{t}^{1/2}}d\bar{t} = 1 - \int_0^{\bar{y}} S(z)dz \tag{19}$$

With $U(0) = 1$. By integrating Eq. (18) by parts and then by substituting Eq. (19), we obtain

$$\frac{F(\bar{y})}{(2\alpha R)^{1/2}} = g(\bar{y}) - \int_0^{\bar{y}} g(\bar{t})S(\bar{y} - \bar{t})d\bar{t} \tag{20}$$

In the dimensional form, the F function is related to the pressure distribution $P(x)$ in the form,

$$\frac{F(x)}{(2\alpha R)^{1/2}} = P(x) - \frac{1}{\alpha R}\int_0^x P(t)\, S\left(\frac{x - t}{\alpha R}\right)dt \tag{21}$$

Similarly, by substituting Eq. (13) into Eq. (1), we may express the F function in terms of the streamline deflection R' on the streamtube,

$$\frac{\alpha F(x)}{(2\alpha R)^{1/2}} = R'(x) - \frac{1}{\alpha R}\int_0^x R'(t)S_1\left(\frac{\alpha R}{x - t}\right)dt \tag{22}$$

Flow disturbances on the streamtube may also be expressed in terms of the corresponding F function by solving integral equations (1) and (22), respectively,

$$\frac{1}{\gamma M_\infty^2}\frac{\Delta p}{p_\infty} = -u = \frac{1}{(2\alpha R)^{1/2}}\left[F(x) + \frac{1}{\alpha R}\int_0^x F(t)K'\left(\frac{x - t}{\alpha R}\right)dt\right] \tag{23}$$

and

$$v = \frac{\alpha}{(2\alpha R)^{1/2}}\left[F(x) + \frac{1}{\alpha R}\int_0^x F(t)K_1'\left(\frac{x - t}{\alpha R}\right)dt\right] \tag{24}$$

Now Eqs. (23) and (24) [or Eqs. (21) and (22)] are exact relations between the flow disturbances and the F function on the streamtube ($r = R$). Since the radius R of the streamtube was chosen arbitrarily, these relations are valid at any distance from the body. Consequently, x and R in Eqs. (23) and (24) may be replaced by y and r, respectively. y is now determined by an exact characteristic equation,

$$x = \alpha(r - R) + y - kF(y)[r^{1/2} - R^{1/2}] - \int_0^y F(t)H\left(\frac{y - t}{\alpha r};\ R\right)dt \tag{25}$$

with

$$H\left(\frac{y - t}{\alpha r};\ R\right) = \frac{M_\infty^2}{2^{1/2}\alpha^{1/2}}\int_R^r \left[K_1'\left(\frac{y - t}{\alpha r}\right) + \frac{(\gamma - 1)M_\infty^2 + 2}{2\alpha^2}K'\left(\frac{y - t}{\alpha r}\right)\right]\frac{dr}{r^{3/2}} \tag{26}$$

Here, R is the local radius of a slender body or the mean radius of a particular streamtube. Now the F function at any location r may be obtained from a known F function at $R(R < r)$ by relating their arguments by Eq. (25)[1,4]. The F function at r is generally not a single valued function at certain regions of its argument. These multiple valued regions are remedied by the presence of shock waves. The flow disturbances at r may be determined from the local F function obtained by the exact relations (23) and (24) with R replaced by r.

By comparing the exact relations (23–25), with Whitham's asymptotic relations (2) and (3), it is observed that the last terms in Eqs. (23–25) are modifications of Whitham's relations, and these terms vanish at large distances. It is also interesting to note that these modification terms may be expanded in power series of $[(y - t)/r]^{1/2}$, and this series expansion is consistent with that suggested by Whitham.[4]

References

[1] Whitham, G. B., "The Flow Pattern of a Supersonic Projectile," *Communications on Pure and Applied Mathematics*, Vol. 5, 1952, pp. 301–348.

[2] Schwartz, I. R., ed., *Second Conference on Sonic Boom Research*, SP-180, NASA, 1968.

[3] Middleton, W. D. and Carlson, H. W., "A Numerical Method for Calculating Near-Field Sonic Boom Pressure Signatures," TN D-3082, Nov. 1965, NASA.

[4] Whitham, G. B., "The Behavior of Supersonic Flow Past a Body of Revolution, Far from the Axis," *Proceedings of the Royal Society*, Ser. A, Vol. 201, 1950, pp. 89–109.

[5] Lighthill, M. M., "Higher Approximations in Aerodynamic Theory," *General Theory of High Speed Aerodynamics*, edited by W. R. Sears, Princeton University Press, Princeton, N. J., 1954, p. 444.

[6] Lighthill, M. J., "Supersonic Flow Past Bodies of Revolution," R&M 2003, 1945, Aeronautical Research Council, London.

[7] Tricomi, F. G., *Integral Equations*, Wiley, New York, 1965, pp. 8–15.

Electron Quench Effects of SF_6 in Air and Argon Plasmas

T. C. Peng* and P. M. Doane†

McDonnell Douglas Corp., St. Louis, Mo.

Introduction

SINCE sulfur hexafluoride (SF_6) has been shown to be effective for reducing electron concentrations in a plasma,[1,2,3] an equilibrium thermochemical study was made on

Received May 6, 1970; revision received July 13, 1970. This research was conducted under the McDonnell Douglas Independent Research and Development Program.

* Associate Scientist. Member AIAA.

† Research Associate. Associate AIAA.

the electron quench effects of SF_6 in air and argon plasmas for wide ranges of temperatures and pressures of re-entry applications. The equilibrium study was made because of its applicability to the re-entry plasma at low altitudes and the establishment of the reaction limits for the nonequilibrium re-entry plasma at high altitudes. The air-SF_6 mixture was selected for Earth re-entry applications, while the argon-SF_6 mixture was selected for comparison with the air-SF_6 mixture and with laboratory experiments using argon plasmas.

Based on minimum Gibbs free energy methods, an initial air SF_6 plasma model consisting of 83 species was used in calculating the equilibrium compositions. The 83 species are: N_2, N_2^+, O_2, O_2^+, O_2^-, O_3, O_3^+, O_3^-, NO, NO^+, NO^-, NO_2, NO_2^+, NO_2^-, NO_3, NO_3^-, N_2O, N_2O^+, N_2O_3, N_2O_4, N_2O_5, N, N^+, O, O^+, O^-, Ar, Ar^+, e^- (29 pure air species), SF_6, SF_6^-, SF_5, SF_5^+, SF_5^-, SF_4, SF_4^+, SF_4^-, SF_3, SF_3^+, SF_3^-, SF_2, SF_2^+, SF_2^-, SF, SF^+, SF^-, S_2F_2, S_3, S_2, S_2^+, F_2, F_2^+, S, S^+, S^-, F, F^+, F^- (29 pure SF_6 species), SOF_2, SO_2F_2, SOF, SO_3, SO_2, SO_2^+, SO_2^-, SO, SO^+, SO^-, SN, SN^+, S_2O, FNO_2, FNO_3, FNO, FO_2, FO, FO^+, FN, FN^+, F_2O, F_2N, F_2N^+, F_3N (25 cross species). Extensive efforts have been made to collect and review the necessary data for internal energy states and heats of formation. Following major assumptions are made:

1) The electronic energy levels and the degeneracies of F^-, O^-, and S^- are assumed the same as those of neutral species (Ne, F, and Cl) with equal number of electrons. Only energy levels up to the electron affinity values of F, O, and S were used. This assumption has previously been made by JANAF.[4]

2) For the species FN^+, FO^+, F_2^+, NS^+, NO^-, SO^+, SO^-, SF^+, SF^-, S_2^+, F_2N^+, SO_2^+, SO_2^-, SF_2^+, SF_2^-, SF_3^+, SF_4^+, SF_5^-, and SF_6^-, the rotational and vibrational energy levels and the electronic ground state degeneracy are assumed to be the same as for the neutral parent species.

3) For the species SF, the heat of formation is determined from the dissociation energy in Ref. 5, and the heat of formation for F based on recent photoionization studies of F_2 dissociation in Ref. 6.

4) For the species SF_5^-, SF_4^-, SF_3^-, SF_2^-, and SF^-, the heat of formation is determined by assuming a zero energy of reaction for $SF_{n+1} + e^- \rightarrow SF_n^- + F$ for $1 \leq n \leq 5$, as indicated by Debolt.[7]

5) The electron affinity value of NO_2 has been reported to be from 1.62 to 4 ev by various investigators.[4,8,9,10] The value adopted in this paper is 4 ev, as quoted by JANAF.

To facilitate the understanding of plasma composition, the number of species in the plasma model was minimized as follows. The equilibrium composition of the initial 83 species model was calculated using a computer program. The output of this program listed the concentrations of all species including the free electrons at specified temperature and pressure values. Each plasma species was evaluated to assess its influence in changing the electron concentration. Selected species were then deleted from the subsequent model, and a new composition calculation was performed. A comparison of the electron concentrations from both calculations was made to verify the equivalency of the two models. The process was repeated until no more species could be deleted without causing more than 5% deviation in electron concentration.

The final result was a 39 species model which is valid for SF_6 mole % from 0.2 to 30 and for temperatures and pressures from 1000 to 10,000°K and 10^{-4} to 10^3 atm, respectively. For pressure ranges of 10^{-4} to 1 atm, usually associated with the conditions in the re-entry vehicle wake flows, only 32 species need to be considered. For the 39 species model, the heats of formation, which have greater sensitivity to the equilibrium composition than the internal energy states, are listed in Table 1.

The argon-SF_6 model consisted of Ar and Ar^+ plus the 29 pure SF_6 species in the air-SF_6 model.

Results and Discussions

For air-SF_6 plasmas, equilibrium compositions have been calculated for pressures ranging from 10^{-4} to 10^3 atm, for temperatures ranging from 1000 to 10,000°K, and for SF_6 mole percent from 0.2 to 30. For the sake of brevity, the results presented in this note will be limited to the pressure range of 10^{-4} to 1 atm associated with re-entry wake studies. However, the general features observed in this pressure range are

Table 1 Heats of formation of species used in final model

Species	ΔH_f at 0°K (Kcal/mol)	Ref.	Species	ΔH_f at 0°K (Kcal/mol)	Ref.
Air species			SF_6 species		
N_2	0.0	By definition	SF_6	−288.46	4
N_2^+	359.3	8	SF_5	−228.0	See[a]
O_2	0.0	By definition	SF_5^-	−303.91	7
O_2^-	−10.0	8	SF_4	−168.4	5
N_2O	20.4	4	SF_4^-	−243.45	7
NO	21.46	4	SF_3	−110.0	12
NO^+	235.17	8	SF_3^-	−183.85	7
NO_2	8.59	4	SF_2	− 51.3	5
NO_2^-	− 83.7	4	SF_2^-	−125.45	7
N	112.5	4	SF	4.1	See[b]
N^+	447.6	11	SF^-	− 69.99	7
O	58.99	4	F_2	0.0	By definition
O^+	373.02	8	S_2	30.8	4
O^-	25.2	4	S_2^+	254.0	11
E^-	0.0	By definition	F	15.45	6
Air SF_6			F^-	− 66.63	See[c]
Cross species			F^+	417.23	See[d]
SO	1.64	4	S	66.1	11
SO_2	− 70.34	4	S^+	304.95	11
SOF_2	−133.87	4	Argon species		
SO_2F_2	−203.17	4	Ar	0.0	By definition
FON	− 15.1	4	Ar^+	363.42	11

[a] Based on energy of reaction given in Ref. 13 and ΔH_f of SF_6 and F given above.
[b] Based on dissociation energy of SF given in Ref. 5 and ΔH_f of S and F given above.
[c] Based on electron affinity of F given in Ref. 11 and ΔH_f of F given above.
[d] Based on ionization potential of F given in Ref. 11 and ΔH_f of F given above.

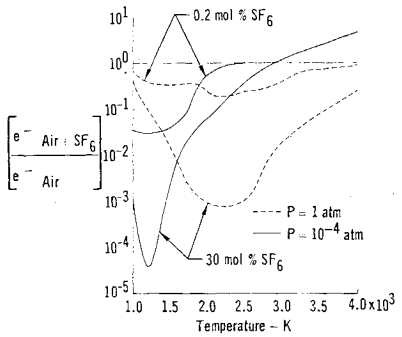

Fig. 1 Effect of SF_6 on equilibrium electron concentrations in air.

also valid for the higher pressure ranges up to 10^3 atm. Typical results for air-SF_6 plasma are shown in Figs. 1 and 2.

Figure 1 illustrates the electron reduction ($e^-_{air+SF_6}/e^-_{air}$) caused by additions of SF_6 in air plasma where the electron concentrations of air plasma (e^-_{air}) were calculated using air species only. The results show the large electron reduction and its strong temperature and pressure dependence for the 30 mole percent SF_6 cases. Detailed examinations of the plasma composition revealed the following physical interpretation. F^- is the primary product causing electron reduction. The other known SF negative ions (SF_5^-, SF_4^-, ..., SF^-) are at least an order of magnitude below the F^- concentration level. Below the maximum reduction temperature, the free electron concentration is the result of a close competition between F^- and NO^+. Above that temperature, the rapid concentration rise, first in S_2^+ and then in S^+, offsets the electron reduction effect of F^-. Eventually, S^+ leads to electron concentrations greater than those observed in pure air plasma. A demonstration of the competition between F^- and other positive ions for the 30 mole % SF_6 case at 1 atm is shown in Fig. 2.

For the 0.2 mole % SF_6 cases, the main feature from Fig. 1 is the relatively small electron reduction with its decreased sensitivity to temperature variations. Detailed plasma composition studies again indicated that F^- is the most dominant negative ion and that close competition exists between F^- and NO^+ for temperatures below the maximum electron reduction range. Furthermore, above the maximum electron reduction temperature, the situations are different for different pressures. At 10^{-4} atm, both S_2^+ and S^+, found important for 30 mole % SF_6 cases, were not significant and F^- simply lost the competition to NO^+, resulting in the electron concentrations equal to that of air plasma after 2500°K. At 1 atm, the electron reduction effect of F^- continues into much higher temperatures and is gradually cancelled by the increasing concentration of S^+ until temperatures at which N^+ and O^+ become dominant.

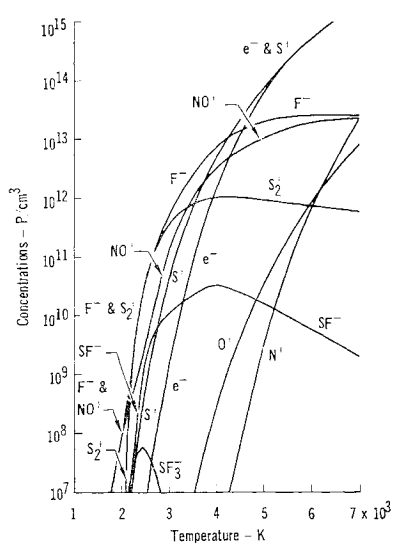

Fig. 2 Ionic species in air + SF_6 plasma with 30 mol % SF_6 at 1 atm pressure.

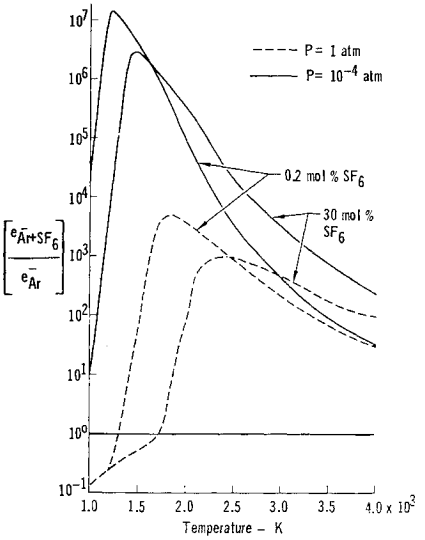

Fig. 3 Effect of SF_6 on equilibrium electron concentrations in argon.

Because many laboratory experiments involving SF_6 use argon as a carrier gas, the equilibrium concentration of argon SF_6 was examined. The effects of SF_6 on the electron concentrations of argon plasma are shown in Fig. 3. As is readily noted, the effect of SF_6 in increasing the electron concentrations in argon is opposite to its effect in air. An examination of the plasma composition showed that the reason for this electron concentration increase is the low ionization potentials of S_2 (9.7 ev) and S (10.3 ev) as compared with that of Ar (15.8 ev). While in air, the low ionization potential of NO (9.25 ev) allows the electrophilic action of F^- to reduce the electron concentration. Since most argon-SF_6 experiments report a decrease in electron concentration with the addition of SF_6, the nature of these experiments is most likely chemically nonequilibrium.

References

[1] Malliaris, A. C. and Libby, D. R., "Testing the Performance of Electrophilic Compounds in High Temperature Flows," AIAA Paper 68-363, San Francisco, Calif. 1968.

[2] Starner, K. E., "Evaluation of Electron Quench Additives in a Subsonic Air Arc Channel," *AIAA Journal*, Vol. 7, No. 12, Dec. 1969, pp. 2357–2358.

[3] Aisenberg, S. and Nydick, S. E., "The Study of Plasma Surrounding Renetry Bodies and Resultant Interaction with Microwave Radiation," AFCRL 60-0239, April 1968, Space Sciences, Inc., Waltham, Mass.

[4] Stull, D. R., "JANAF Thermochemical Tables," with Addendums 1–3, August 1965–1968, The Dow Chemical Co., Midland, Mich.

[5] McBride, B. J. et al., "*Thermodynamic Properties to 600 K for 210 Substances Involving the First 18 Elements*," SP-3001, NASA, 1963.

[6] Dibler, V., Waler, J., and McCulloh, K., "Dissociation Energy of Fluorine," *Journal of Chemical Physics*, Vol. 50, May, 15, 1969, pp. 4592–93; also "Photoionization Study of the Dissociation Energy of Fluorine and the Heat of Formation of Hydrogen Fluoride," *Journal of Chemical Physics*, Vol. 51, Nov. 15, 1969, pp. 4230–35.

[7] DeBolt, H. E., "Basic Considerations in Wake Quench," Wake Quench/Seed Specialists Meeting, Aerospace and SAMSO, Norton AFB, Oct. 1967, San Bernardino, Calif.

[8] Gilmore, F. R., "Basic Energy Level and Equilibrium Data for Atmospheric Atoms and Molecules," AD 650-470, March 1967, Rand Corp., Santa Monica, Calif.

[9] Sutton, E. A., "Chemistry of Electron in Pure-Air Hypersonic Wakes," *AIAA Journal*, Vol. 6, No. 10, Oct. 1968, pp. 1873–1882.

[10] Branscomb, L. M., "A Review of Photodetachment and Related Negative Ion Processes Relevant to Aeronomy," *Annales de Geophysique*, Vol. 20, 1964, p. 88.

[11] Wagman, D. D. et al., "Selected Values of Chemical Thermodynamic Properties," TN 270-3, Jan. 1968, National Bureau of Standards.

[12] Wilkins, R. L., "Thermodynamics of SF_6 and Its Decomposition and Oxidation Products," TR 0158 (3240-20)-19, July 1968, Aerospace Corporation, El Segundo, Calif.

[13] Bott, J. and Jacobs, T., "Shock-Tube Studies of Sulfur Hexafluoride," *Journal of Chemical Physics*, Vol. 50, May 1969, pp. 3850–55.

A Tractable Method for Estimating Atomic and Molecular Transport Coefficients

R. L. Fox* and R. S. Bernard*

Sandia Laboratories, Albuquerque, N. Mex.

TO calculate the flow in the vicinity of an ablating or transpiration cooled surface, one often requires the values of the transport coefficients of the various species injected into the boundary layer. Sufficient experimental data does not exist to obtain parameters needed for a semiempirical determination of these transport coefficients. A method of obtaining transport coefficients without recourse to experimental data would thus be of great value. Such methods have been studied in the past by other investigators.[1]

The purpose of this Note is to present a method of calculating transport coefficients, which is simple enough to be carried out quickly and without the use of a computer. Comparison of transport coefficients obtained using this method with experimental data show agreement which is generally as good as those obtained from more elaborate computation.

The interaction between two neutral molecules is taken to be of the form of a dispersion potential $V(r) = -A/r^6$,[2a] where r is the interparticle separation, and A is a constant for a given set of molecules. The apparent collision radius for the interaction is obtained by letting the potential be proportional to the gas temperature T. The constant of proportionality has previously been studied,[3] where it has been shown that transport coefficients depend weakly on the proportionality constant. As shown below, the present method is independent of the proportionality constant, but introduces another parameter which will be discussed later.

It is assumed that for some gas temperature T_1 the collision radius equals the root mean square radius of the outer shell electrons in the molecule, r_{ms}. With this assumption, the collision cross section σ becomes

$$\sigma = \pi \bar{r}^2 (T_1/T)^{1/3} \tag{1}$$

The transport coefficients can be written in terms of the mean square radius as

$$\mu \times 10^7 = 133.46 T^{5/6}(M^*)/(T_1^{1/3} r_{ms}) \tag{2}$$

$$D \times 10^7 = 3285 T^{11/6}/(r_{ms} p T_1^{1/3} M^*) \tag{3}$$

and

$$K \times 10^7 = 248.6 T^{5/6}/(M^* r_{ms} T_1^{1/3}) \tag{4}$$

where μ is the viscosity in g/cm sec, D is the diffusion coefficient in cm²/sec, K is the translational thermal conductivity in cal/cm sec °K, p is the pressure in atmospheres,

Received May 4, 1970; revision received, August 21, 1970.

This work was supported by the United States Atomic Energy Commission.

* Technical Staff Members, Aero-Fluid Dynamics Division, Sandia Laboratories, Albuquerque, N. Mex.

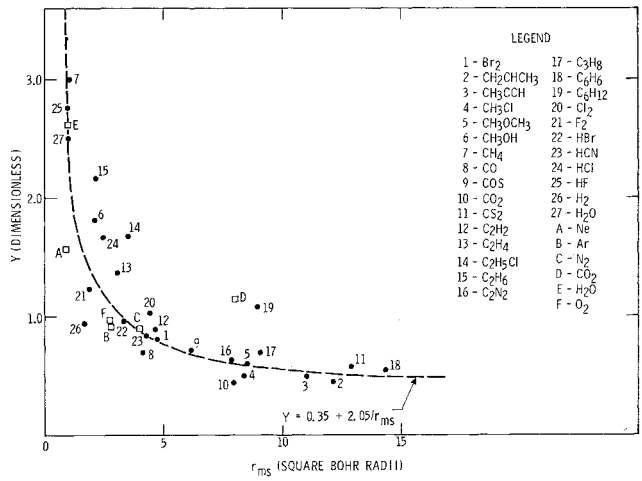

Fig. 1 Data used to obtain T_1 as a function of r_{ms}.

M^* is the reduced molecular mass in a.m.u., T_1 and T are in °K, and r_{ms} is in square Bohr radii, where the Bohr radius is 0.529 angstroms.

Calculation of the mean square radius for a single component monatomic gas using screening constants is straightforward.[2b] For a single component polyatomic gas the mean square radius can be obtained by averaging the screening constants and effective principal quantum numbers of the electron in the molecule's far field and near field. The far-field values are obtained by considering the molecule as an atom of nuclear charge equal to the sum of the atomic nuclear charges. The near-field values are obtained by averaging the effective quantum numbers and effective nuclear charges of all the atoms in the molecule.

This method of obtaining mean square molecular radii neglects the effects of inelastic processes and interactions caused by polar molecules. These effects are important in developing a rigorous theory, but can be neglected for the range of accuracies expected from the method developed in this Note.

The extension to multicomponent mixtures can be carried out by applying the approximate relation between the interaction coefficients of unlike molecules with the coefficients for like molecules.[2c] When this relation is applied, an expression relating the mean square radii is obtained. For molecules of type γ and β this relation is $(r_{ms})^2_{\gamma\beta} = (r_{ms})_\gamma (r_{ms})_\beta$.

The choice of a value for T_1 will now be discussed. The value of the temperature at which the collision cross section is equal to πr_{ms}, i.e., T_1, should decrease with increasing r_{ms} due to the increased volume over which the valence electrons are distributed in the latter case. The dependence of T_1 on r_{ms} was obtained by calculating the transport coefficient assuming $T_1 = 1000$°K for a variety of atomic and molecular gases for which experimental data exist. The ratio of the theoretical to the experimental values for each coefficient were plotting against r_{ms}. Figure 1 is a plot of this ratio Y

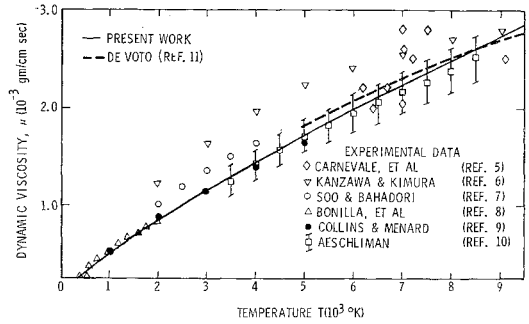

Fig. 2 Comparison of theoretical and experimental viscosities of monatomic argon.